Vibrational spectroscopic study of the mineral pitticite Fe, AsO_4, SO_4, H_2O

Ray L. Frost,[•] Yunfei Xi, Keqin Tan, Graeme J. Millar, Sara J. Palmer

Chemistry Discipline, Faculty of Science and Technology, Queensland University of Technology, GPO Box 2434, Brisbane Queensland 4001, Australia.

Abstract

Some minerals are colloidal and show no X-ray diffraction patterns. Vibrational spectroscopy offers one of the few methods for the determination of the structure of these minerals. Among this group of minerals is pitticite, simply described as (Fe, AsO_4, SO_4, H_2O). In this work, the analogue of the mineral pitticite has been synthesised. The objective of this research is to determine the molecular structure of the mineral pitticite using vibrational spectroscopy. Raman and infrared bands are attributed to the AsO_4^{3-} , SO_4^{2-} and water stretching and bending vibrations. The Raman spectrum of the pitticite analogue shows intense peaks at 845 and 837 cm^{-1} assigned to the AsO_4^{3-} stretching vibrations. Raman bands at 1096 and 1182 cm^{-1} are attributed the SO_4^{2-} antisymmetric stretching bands. Raman spectroscopy offers a useful method for the analysis of such colloidal minerals.

Keywords: Raman spectroscopy, pitticite, arsenate, sulphate, scorodite, känkite

[•] Author to whom correspondence should be addressed (r.frost@qut.edu.au)
P: +61 7 3138 2407 F: +61 7 3138 1804

Introduction

Pitticite is an amorphous hydrous ferric sulphate formed [1] as a late secondary mineral typically formed by oxidation of earlier arsenic-bearing minerals [2]. The mineral is typically found in mine waste dumps and even in tailings dams [1, 3-5]. The structure of the mineral is not known and the mineral is X-ray non-diffracting. The mineral is white to yellow-brown but may display a red colour because of deep internal reflections [6, 7]. The name pitticite has validity only as a generic name for gel-like Fe^{3+} arsenate minerals of varying composition [1]. As such the mineral should be able to be readily synthesised. This is an objective of this research.

The removal of arsenic from the environment is of importance both in industrial wastes, aqueous systems and in spoilt soils [8, 9]. Methodology for waste water treatment is an ongoing task [10]. The actual speciation of arsenic in aqueous media and soils is important [6, 11] . There have been some studies on the application of Raman spectroscopy to identify arsenic containing minerals [7]. Filippi et al. identified arsenate bearing minerals including scorodite, kankite and amorphous ferric arsenate [7]. These workers labelled amorphous ferric arsenate as pitticite but according to Anthony et al. [12] the mineral pitticite contains sulphate as well as arsenate in the mineral in a rough ratio of 3:1. Gomez et al. studied the Raman spectroscopy of the synthesised analogues of scorodite and its formation [13, 14]. Such studies are of importance in gold recovery [13]. These researchers reported a synthesised mineral equivalent to pitticite.

In Australia, arsenic compounds such as sodium arsenate, arsenic trichloride and arsenic pentachloride are used as tick control chemicals in cattle dips. This results in the contamination of soils around dip sites with arsenic compounds [15]. If the soils are in anyway acidic then the amorphous mineral pitticite will form. There is a need to be able to identify consequential mineral formation in soils. There are many cattle dips in and around Brisbane. Many cattle dip sites have been converted to parklands and house sites. Often the soil is toxic and is a health risk to families living near such sites. To remove arsenic from soils, the arsenic must be oxidised to arsenate followed by reaction with appropriate cations in the soils. The arsenate then reacts with Fe^{3+} of Al^{3+} to form arsenate containing minerals

such as pitticite and related minerals scorodite. It is important to be able to remove and immobilise arsenic. This research forms part of a systematic study of arsenic forming compounds in soils.

Minerals such as pitticite are formed through the reaction of acid sulphate solutions with already formed arsenate minerals. Because of the known and ill-defined structure of these minerals, it is very important to undertake structural studies. Due to the amorphous nature of pitticite the application of vibrational spectroscopy is very important. Only through vibrational spectroscopy can any concepts of the molecular structure of the mineral be determined. The minerals act as a sink for both sulphur and arsenate waste mine dumps. Further the minerals have been found in old or ancient burial sites. Some vibrational spectroscopic studies of the related arsenate containing minerals have been undertaken [7]. Some assignment of bands was undertaken and the spectra were simply reported without any explanation [7]. There is a vital need to study the molecular structure of these types of minerals in more detail.

The reason for this research is that minerals such as pitticite are found in old mine sites. A comprehensive review of arsenic speciation and mobility has been provided [16] Further, the formation of pitticite can be used as the basis for arsenic accumulation [6, 7]. Therefore, this research focuses on the spectroscopic determination of pitticite and consequential molecular structure. Raman spectroscopy has proven very useful for the study of minerals [17-20]. Indeed Raman spectroscopy has proven most useful for the study of diagenetically related minerals as often occurs with minerals containing arsenate and sulphate groups. Raman spectroscopy is especially useful when the minerals are X-ray non-diffracting or poorly diffracting and very useful for the study of amorphous and colloidal minerals. Pitticite is a mineral which falls into this category.

This paper is a part of systematic studies of vibrational spectra of minerals of secondary origin in the oxide supergene zone. In this work we attribute bands at various wavenumbers to vibrational modes of pitticite using Raman spectroscopy and relate the spectra to the structure of the mineral.

Experimental

Mineral Synthesis

The chemicals were purchased as follows: disodium hydrogen arsenate heptahydrate, sodium sulphate decahydrate and iron(III) chloride hexahydrate are from Sigma-Aldrich.To prepare pitticite $Fe_{2.95}(AsO_4)_{1.63}(SO_4)$, 14.82g Na_2HAsO_4 and 11.20g Na_2SO_4 were dissolved in 110ml deionized water as solution 1. 25.68g $FeCl_3$ were dissolved in 100ml deionized water as solution 2. Solution 1 was slowly dropped into solution 2 under mechanical agitation. The final pH of the resulting mixture was raised with 1 M NaOH to pH 3 causing the spontaneous precipitation. The precipitated slurry was continuously agitated at constant pH for another 8 hours. Paper filter was used to collect solid material which was washed four times with deionized water. The wet cake was finally dried at 105°C overnight.

The mineral pitticite was supplied by the Mineralogical Research Company and originated from The White caps Miner, Nye County, Nevada. Details of the mineral have been published (page 468) [21].

Raman spectroscopy

Gel-like crusts of pitticite were placed on a polished metal surface on the stage of an Olympus BHSM microscope, which is equipped with 10x, 20x, and 50x objectives. The microscope is part of a Renishaw 1000 Raman microscope system, which also includes a monochromator, a filter system and a CCD detector (1024 pixels). The Raman spectra were excited by a Spectra-Physics model 127 He-Ne laser producing highly polarised light at 633 nm and collected at a nominal resolution of 2 cm^{-1} and a precision of ± 1 cm^{-1} in the range between 100 and 4000 cm^{-1}. Power at the sample was 0.1 watts. Repeated acquisition on the crystals using the highest magnification (50x) was accumulated to improve the signal to noise ratio in the spectra. Spectra were calibrated using the 520.5 cm^{-1} line of a silicon wafer.

Infrared spectroscopy

Infrared spectra were obtained using a Nicolet Nexus 870 FTIR spectrometer with a smart endurance single bounce diamond ATR cell. Spectra over the 4000–525 cm^{-1} range were

obtained by the co-addition of 128 scans with a resolution of 4 cm^{-1} and a mirror velocity of 0.6329 cm/s. Spectra were co-added to improve the signal to noise ratio.

Band component analysis was undertaken using the Jandel 'Peakfit' (Erkrath, Germany) software package which enabled the type of fitting function to be selected and allowed specific parameters to be fixed or varied accordingly. Band fitting was undertaken using a Lorentz-Gauss cross-product function with the minimum number of component bands used for the fitting process. The Lorentz-Gauss ratio was maintained at values greater than 0.7 and fitting was undertaken until reproducible results were obtained with squared correlations (r^2) greater than 0.995. Band fitting of the spectra is quite reliable providing there is some band separation or changes in the spectral profile.

Results and discussion

Background

The mineral pitticite contains both sulphate and arsenate anions. Therefore the spectroscopy of the mineral will in part on the identification of these two anions. The T_d symmetry is characteristic for both free units $(SO_4)^{2-}$ and $(AsO_4)^{3-}$ ions. In dilute aqueous solutions, $(SO_4)^{2-}$ ions exhibit the symmetric stretching vibration (A_1, ν_1), 983 cm^{-1} – Raman active, the doubly degenerate bending vibration (E, ν_2), 450 cm^{-1} – Raman active, the triply degenerate antisymmetric stretching vibration (F_2, ν_3), 1105 cm^{-1} – Raman and infrared active, and the triply degenerate bending vibration (F_2, ν_4), 611 cm^{-1} – Raman and infrared active. Any symmetry lowering may activate some or all vibrations in both Raman and IR and cause the splitting of degenerate vibrations [22-24] . Fundamental vibrational modes for $(AsO_4)^{3-}$ are the symmetric stretching vibration (A_1, ν_1), 837 cm^{-1} – Raman active, the doubly degenerate bending vibration (E, ν_2), 349 cm^{-1} – Raman active, the triply degenerate antisymmetric stretching vibration (F_2, ν_3) – 878 cm^{-1} – Raman and infrared active, and the triply degenerate bending vibration (F_2, ν_4), 463 cm^{-1} – Raman and infrared active. Similarly, as in the case of sulfate ions, any symmetry lowering may cause Raman and infrared activation of some or all vibrations and the splitting of degenerate vibrations [23, 25].

S.D. Ross in Farmer's treatise [26] reported the infrared spectrum of beudantite (Table 18.IX page 433). This table compares the infrared spectra of minerals from the alunite-jarosite supergroups. Ross [26] reported infrared bands of these minerals at 985, 1006 cm^{-1} (ν_1), 430, 466 cm^{-1} (ν_2), 1078, 1160 cm^{-1} (ν_3), 600, 625 and 670 cm^{-1} (ν_4). OH vibrations were reported

at 3420 and 525 cm^{-1} attributed to the stretching and bending of the OH units. The sulphate stretching mode for Cu-beudantite [27] was listed as 1010 cm^{-1} and the ν_2 bending modes were reported at 620, 662 and 687 cm^{-1}. The arsenate stretching bands were listed as occurring at 729, 813, 821, 851 and 870 cm^{-1}. The arsenate bending modes were not reported, no doubt because these bands occurred outside the detection limits of the instrument.

Spectroscopy

The Raman spectrum of the synthetic pitticite over the 100 to 4000 cm^{-1} range is shown in Figure 1a. The corresponding infrared spectrum over the 550 to 4000 cm^{-1} range is displayed in Figure 1b. These figures show the relative intensities of bands within each spectrum and also show a comparison of the intensities between the two spectroscopic techniques. There are obvious regions in the spectra where no bands are found. As a consequence the spectra are subdivided into sections as a function of the type of vibration being observed.

The Raman spectrum of pitticite in the 600 to 1300 cm^{-1} region is reported in Figure 2a. The infrared spectrum in the 700 to 1300 cm^{-1} region is reported in Figure 2b. This spectral region is where the stretching vibrations of the sulphate and arsenate anions are found. The Raman spectrum shows two peaks at 845 and 837 cm^{-1} assigned to the AsO_4^{3-} stretching vibrations. A resolved component band at 916 cm^{-1} is also observed. Although the position of this band is very low for the sulphate anion, this band may be the SO_4^{2-} symmetric stretching vibration. In this work we have synthesised pitticite according to the formula given by Anthony et al. [12]. According to Anthony et al. the ratio of sulphate to arsenate is 1:3. Thus it could be expected that the intensity of the bands for arsenate anion would be more intense.

The Raman bands at 1096 and 1182 cm^{-1} are attributed the SO_4^{2-} antisymmetric stretching bands. Infrared bands are observed at 805 and 860 cm^{-1} with component bands at 747 and 915 cm^{-1}. The infrared bands at 805 and 860 cm^{-1} are assigned to the AsO_4^{3-} antisymmetric and symmetric stretching modes. The infrared bands at 1045, 1076, 1121 and 1194 cm^{-1} are attributed to the SO_4^{2-} antisymmetric stretching bands. A comparison may be made with the spectra of the natural pitticite. The Raman spectrum of natural pitticite is dominated by a very intense sharp band at 983 cm^{-1} assigned to the SO_4^{2-} symmetric stretching mode. The

same vibrational mode is observed in the infrared spectrum as a sharp band at 983 cm^{-1}. A strong Raman band at 1041 cm^{-1} is observed and is assigned to the SO_4^{2-} antisymmetric stretching mode. Other bands at 1102, 1118, 1147 and 1215 cm^{-1} are attributed also to this vibrational mode. In the infrared spectrum, these antisymmetric stretching modes are found at 1012, 1056, 1107 and 1146 cm^{-1}.

The Raman spectrum in the 100 to 600 cm^{-1} region is reported in Figure 3a. The infrared spectrum in the 550 to 700 cm^{-1} region is shown in Figure 3b. This spectral region contains the peaks associated with the bending modes of the sulphate and arsenate anions. A broad Raman band is observed at 647 cm^{-1} and is assigned to the $\nu_4 (SO_4)^{2-}$ bending mode. An additional band at 504 cm^{-1} may also be attributed to this vibrational mode. In the infrared spectrum these vibrational modes show much greater intensity. Infrared bands are observed at 622, 631, 638 and 653 cm^{-1}. The Raman bands at 401, 428 and 457 cm^{-1} are attributable to the doubly degenerate $\nu_2 (SO_4)^{2-}$ bending mode. The multiplicity of Raman bands in the 260 to 360 cm^{-1} region are attributed to the ν_2 and ν_4 AsO_4^{3-} bending modes. The bands below 260 cm^{-1} may be described as lattice vibrations.

The Raman spectrum of pitticite in the OH stretching region is reported in Figure 4a and the infrared spectrum is displayed in Figure 4b. The Raman spectrum in this spectral region suffers from a lack of intensity. This is not unexpected as water is a very poor Raman scatterer. Raman bands may be curve resolved at 2723, 3060, 3186, 3327 and 3490 cm^{-1}. These bands are attributed to water stretching vibrations in different hydrogen bonding states. In the infrared spectrum bands are observed at 2675, 2851, 3013, 3232 and 3457 cm^{-1}. The bands at the lower wavenumber represent water in strong hydrogen bonds whilst the higher wavenumber bands belong to water in less strongly hydrogen bonding. A comparison may be made with the natural pitticite. Four Raman bands are found at 3167, 3258, 3411 and 3550 cm^{-1}. In the infrared spectrum, bands are observed at 3123, 3209, 3376 and 3487 cm^{-1}. The observation of multiple hydroxyl stretching wavenumbers reflects the hydrogen bond distances between the OH units and the adjacent AsO_4 units [28]. Studies have shown a strong correlation between OH stretching frequencies and both the O···O bond distances and the H···O hydrogen bond distances. The work of Libowitzky showed that a regression

function can be employed relating the above correlations with regression coefficients better than 0.96 [28]. The function is $\nu_1 = 3592\text{-}304x109\exp(-d(O\text{-}O)/0.1321)$ cm^{-1}.

Mechanism of formation of scorodite and kankite

The formation of the mineral pitticite offers a mechanism for the formation of other minerals such as scorodite $FeAsO_4 \cdot 2H_2O$ and kankite $FeAsO_4 \cdot 3.5H_2O$ [16, 29]. The reactions below show the envisaged chemical reactions. If anions other than the arsenate anion, are present, then other minerals may also form. Included in these minerals are beudantite $PbFe_3^{3+}(AsO_4)(SO_4)(OH)_6$, bukovskyite $Fe_3^{3+}(AsO_4)(SO_4)(OH) \cdot 7H_2O$, gartrellite $Pb[(Cu,Fe^{2+})(Fe^{3+}, Zn, Cu)] (AsO_4)(CO_3,H_2O)_2$, sarmientite $Fe_2^{3+}(AsO_4)(SO_4)(OH) \cdot 5H_2O$, and zykaite $Fe_4^{3+}(AsO_4)_3(SO_4)(OH) \cdot 15H_2O$. Each of these minerals act as accumulators of arsenate anions and function as arsenate sinks.

The formation of these minerals is dependent upon the pH, the ion concentrations and the temperature [16, 29-32]. The following reactions are envisaged. These reactions show the formation of scorodite and kankite. Similar reactions are possible for the minerals listed above.

$$Fe, AsO_4, SO_4, H_2O \rightarrow FeAsO_4 \cdot 2H_2O \text{ (scorodite)} + FeSO_4 \cdot 4H_2O$$

$$Fe, AsO_4, SO_4, H_2O \rightarrow FeAsO_4 \cdot 3.5H_2O \text{ (kankite)} + FeSO_4 \cdot 4H_2O$$

The difference between scorodite and kankite is simply the number of waters of hydration. The minerals nucleate and crystallise from these pitticite colloidal solutions.

The formation of these minerals offers a mechanism for arsenate waste water treatment and in soil remediation.

Conclusions

Pitticite is an example of a mineral which resembles a gel and shows no X-ray diffraction patterns. The application of vibrational spectroscopy is of importance as it offers one of the only methods for the assessment of the molecular structure of the mineral. In this work we

have synthesised the analogue of the mineral pitticite. The application of the formation of pitticite lies in arsenate accumulation and storage.

The Raman spectrum of the pitticite analogue is dominated by bands at 845 and 837 cm^{-1} assigned to the AsO_4^{3-} stretching vibrations. Infrared bands at 805 and 860 cm^{-1} are assigned to the AsO_4^{3-} antisymmetric and symmetric stretching modes. It is expected that the intensity of the arsenate bands would be stronger than the sulphate bands because the ration of arsenate to sulphate is 3:1. The observation of multiple bands in the ν_4 $(SO_4)^{2-}$ spectral region supports the concept of reduction in symmetry of the sulphate anion in these structures. A comparison is made with the spectra of the natural pitticite. Vibrational spectroscopy is important in the assessment of the molecular structure of the pitticite gel, especially when the mineral is non-diffracting.

Acknowledgments

The financial and infra-structure support of the Queensland University of Technology, Chemistry Discipline is gratefully acknowledged. The Australian Research Council (ARC) is thanked for funding the instrumentation.

References

[1] P.J. Dunn, Mineralogical Magazine 46 (1982) 263.
[2] A. Kopriva, J. Zeman, O. Sracek, Natural Arsenic in Groundwater: Occurrence, Remediation and Management, Proceedings of the Pre-Congress Workshop "Natural Arsenic in Groundwater (BWO 06)", International Geolog (2005) 49.
[3] J. Jansa, F. Novak, J. Sevcu, K. Hora, Neues Jahrbuch fuer Mineralogie, Monatshefte (1974) 330.
[4] R. Kraemer, Neues Jahrbuch fuer Mineralogie, Geologie und Palaeontologie, Abhandlungen, Abteilung A: Mineralogie, Petrographie (1915) 331.
[5] G. Schnorrer, A. Kronz, W. Liessmann, A. Kehr, Aufschluss 60 (2009) 29.
[6] M. Filippi, V. Golias, Z. Pertold, Environmental Geology (Berlin, Germany) 45 (2004) 716.
[7] M. Filippi, V. Machovic, P. Drahota, V. Bohmova, Applied Spectroscopy 63 (2009) 621.
[8] V.K. Gupta, I. Ali, Environmental Science and Technology 42 (2008) 766.
[9] V.K. Gupta, Suhas, Journal of Environmental Management 90 (2009) 2313.
[10] V.K. Gupta, P.J.M. Carrott, M.M.L.R. Carrott, Critical Reviews in Environmental Science and Technology 39 (2009) 783.
[11] M. Filippi, B. Dousova, V. Machovic, Geoderma 139 (2007) 154.
[12] J.W. Anthony, R.A. Bideaux, K.W. Bladh, M.C. Nichols, Handbook of Mineralogy. Mineral Data Publishing, Tuscon, Arizona, USA, 1995.
[13] M.A. Gomez, H. Assaaoudi, L. Becze, J.N. Cutler, G.P. Demopoulos, Journal of Raman Spectroscopy 41 (2010) 212.
[14] M.A. Gomez, L. Becze, M. Celikin, G.P. Demopoulos, Journal of Colloid and Interface Science 360 (2011) 508.
[15] J.O. Okonkwo, Bull Environ Contam Toxicol 79 (2007) 380.
[16] P. Drahota, M. Filippi, Environment International 35 (2009) 1243.
[17] R.L. Frost, S.J. Palmer, J. Mol. Struct. 988 (2011) 47.
[18] R.L. Frost, S.J. Palmer, H.J. Spratt, W.N. Martens, J. Mol. Struct. 988 (2011) 52.
[19] S.J. Palmer, R.L. Frost, J. Mol. Struct. 994 (2011) 283.
[20] G. Udayabashakar Reddy, R. Ramasubba Reddy, Y. Nakamura, S. Lakshmi Reddy, T. Endo, R.L. Frost, J. Mol. Struct. 994 (2011) 238.
[21] J.W. Anthony, R.A. Bideaux, K.W. Bladh, M.C. Nichols, Handbook of Mineralogy Vol.IV. Arsenates, phosphates, vanadates - Mineral Data Publishing, Tucson, Arizona. Mineral data Publishing, Tucson, Arizona, 2000.
[22] H.A. Szymanski, L. Marabella, J. Hoke, J. Harter, Appl. Spectrosc. 22 (1968) 297.
[23] S.C.B. Myneni, Rev. Mineral 40 (2000) 113.
[24] M.D. Lane, American Mineralogist 92 (2007) 1.
[25] P. Keller, Neues Jb. Mineral. Mh. 11 (1971H) 491.
[26] V.C. Farmer, Mineralogical Society Monograph 4: The Infrared Spectra of Minerals. 1974.
[27] J. Sejkora, J. Skovira, J. Cejka, J. Plasil, Journal of Geosciences 54 (2009) 355.
[28] E. Libowitzky, Monatsh. Chem. 130 (1999) 1047.
[29] P. Drahota, M. Mihaljevic, T. Grygar, J. Rohovec, Z. Pertold, Environmental Earth Sciences 62 (2011) 429.
[30] P. Drahota, T. Paces, Z. Pertold, M. Mihaljevic, P. Skrivan, Science of the Total Environment 372 (2006) 306.
[31] P. Drahota, Z. Pertold, M. Pudilova, Journal of the Czech Geological Society 50 (2005) 19.

[32] P. Drahota, J. Rohovec, M. Filippi, M. Mihaljevic, P. Rychlovsky, V. Cerveny, Z. Pertold, Science of the Total Environment 407 (2009) 3372.

List of Figures

316

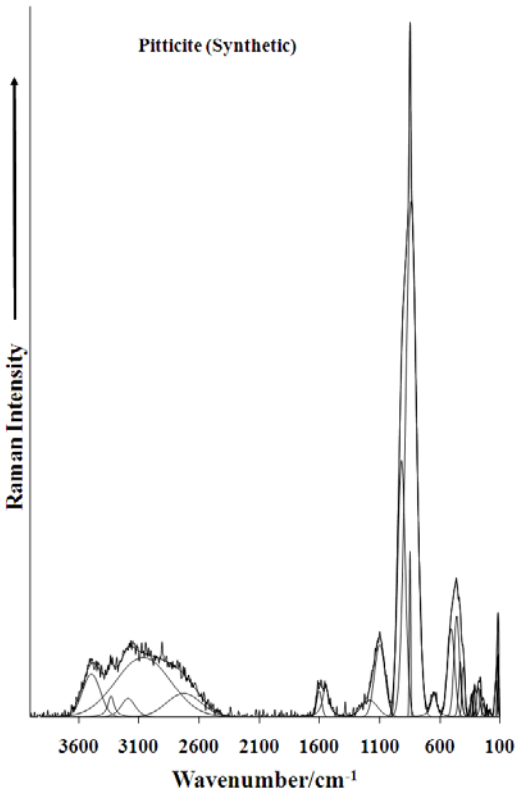

Figure 1a

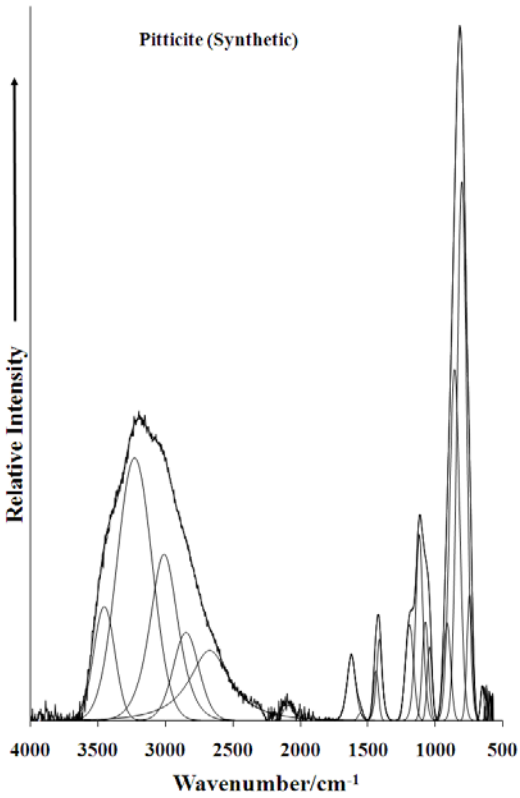

Figure 1b

317

318

319

320

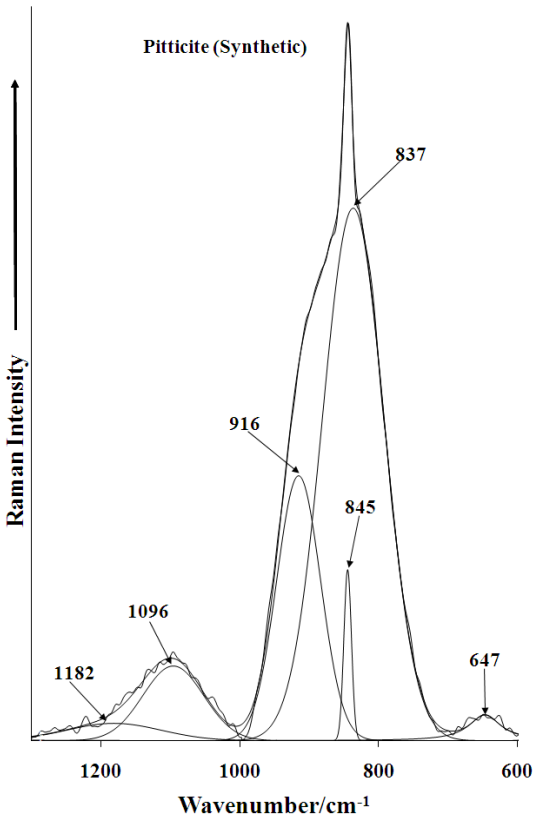

Figure 2a

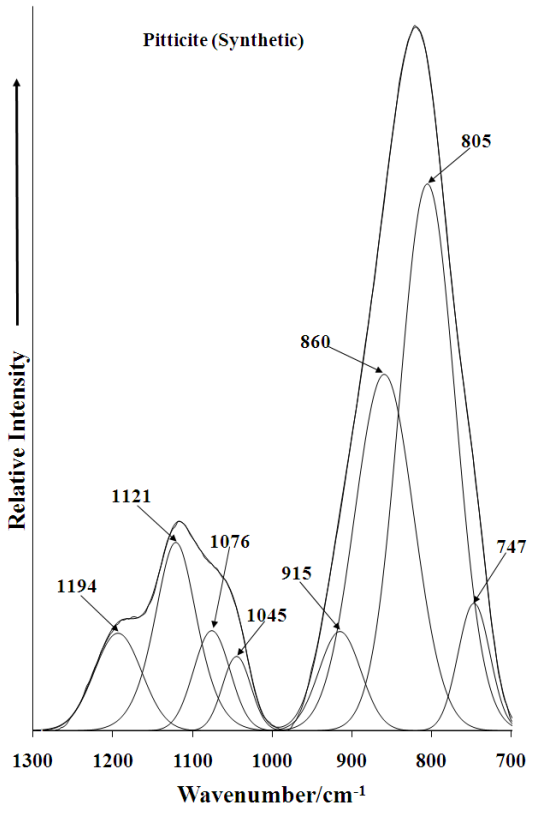

Figure 2b

321

322

323

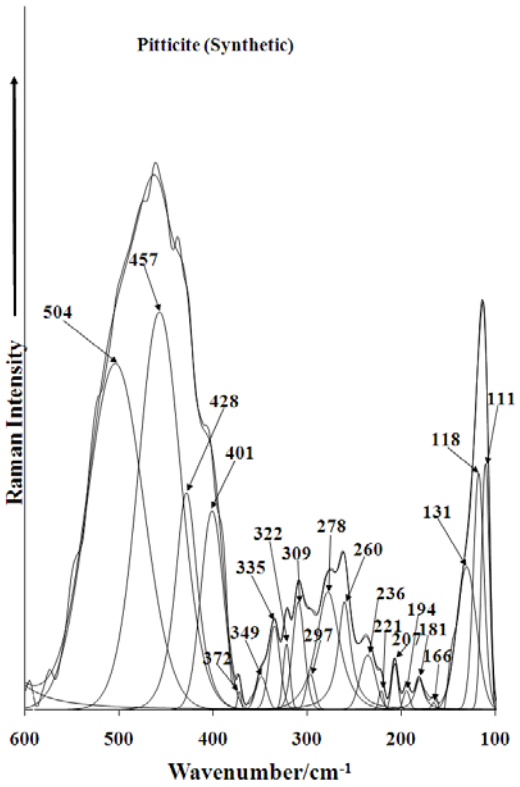

Figure 3a

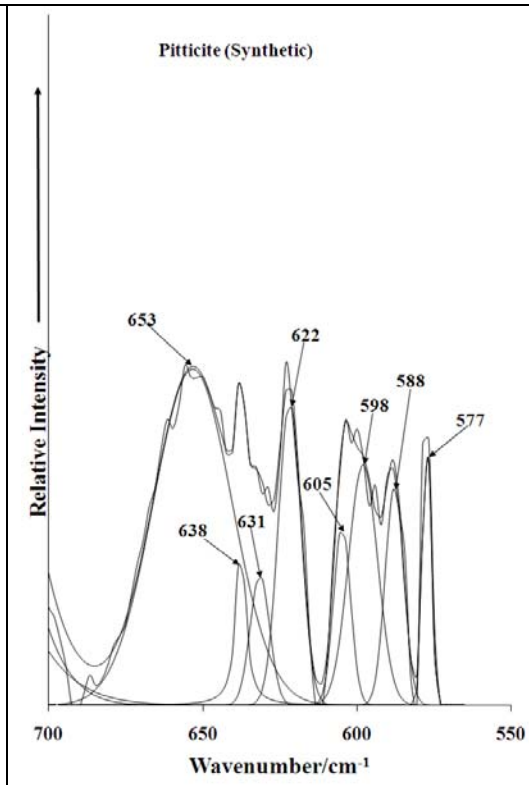

Figure 3b

328

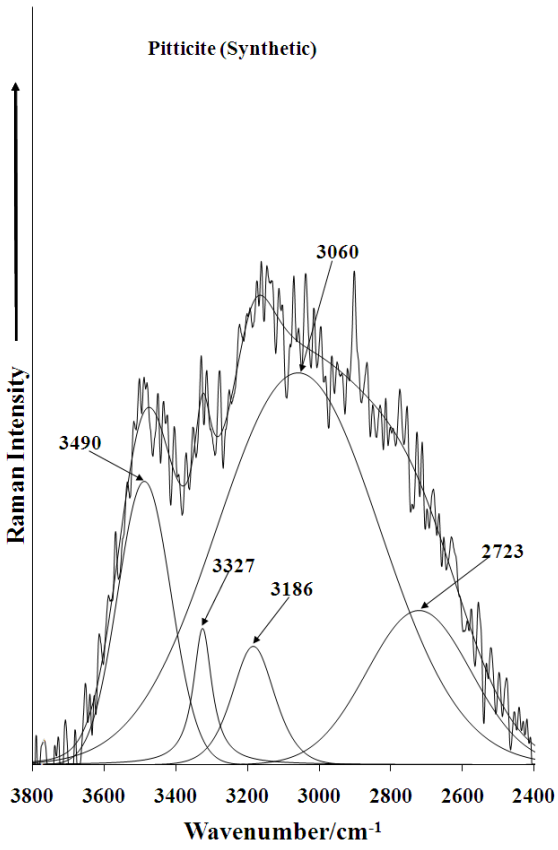

Figure 4a

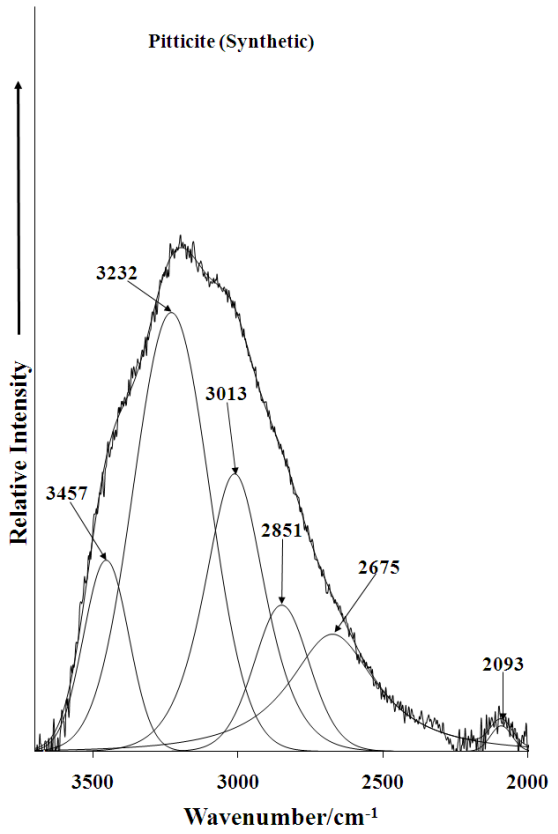

Figure 4b

329

330

331